ISSN: 2230-9926

Available online at http://www.journalijdr.com

IJDR

International Journal of Development Research
Vol. 09, Issue, 04, pp. 26890-26896, April, 2019

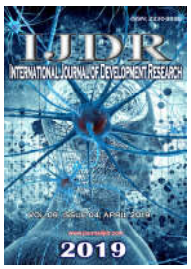

RESEARCH ARTICLE OPEN ACCESS

AN ALGORITHM FOR THE ENHANCEMENT OF THERMODILUTION SIGNALS

***[1]Maxwell D. B. Melo, [1]Humberto X. Araujo, [1]Sergio R. Gobira and [2]Adson F. da Rocha**

[1]Federal University of Tocantins, Faculty of Electrical Engineering, Palmas, Brazil
[2]University of Brasilia, Faculty of Electrical Engineering, Brasília, Brazil

ARTICLE INFO

Article History:
Received 29th January, 2019
Received in revised form
27th February, 2019
Accepted 09th March, 2019
Published online 29th April, 2019

Key Words:
Thermodilution, Deconvolution, Recovery, Cardiac output, Ejection fraction.

ABSTRACT

This study aimed to develop and evaluate an algorithm for enriching the thermodilution signal. The method proposed presents an improvement of previous works in the literature in terms of precision, convergence and computational effort. The algorithm proposed is a deconvolution method that works without the need for precise knowledge of the transfer function of the temperature sensor in the Swan-Ganz catheter. In this method, the prior knowledge of the nature of the sensor response and a specific characteristic of the actual thermodilution signal is used, to estimate the response of the sensor, and then to determine a better estimate for the actual signal.

Citation: Maxwell D. B. Melo, Humberto X. Araujo, Sergio R. Gobira and Adson F. da Rocha. 2019. "An algorithm for the enhancement of thermodilution signals", *International Journal of Development Research*, 09, (04), 26890-26896.

INTRODUCTION

The heart and the vascular bed form a system for distribution of gas and nutrients, and extraction of carbon dioxide and metabolites generated by the human metabolism, helping several defense systems and aiding in the distribution of leukocytes and substances related to blood coagulation [1]. Due to its great importance, there are many devices for assessing the condition of the cardiovascular system. The primary goal of this work is the development of an algorithm to improve the quality of temperature measurement by the Swan-Ganz catheter sensor, using a technique called deconvolution. The thermodilution method allows for the measurement of several hemodynamic parameters in patients with cardiovascular diseases. Determining cardiac output and ejection fraction can help predict many diseases, including estimating the risk of sudden death (ejection fraction <0.2), which is becoming more common. In the operation of the human heart, the left or right ventricle of the heart is filled with blood during the diastole. After the ventricle is filled, the contraction (or systole) begins, and a fraction of the blood is ejected to the lungs and to the peripheral circulation. The ejection fraction is the ratio between the volume of blood that is ejected and the maximum volume of blood when the ventricle was full (at the end of the diastole). The cardiac output is the volume (usually in L/min) of blood pumped by the heart in one minute. The thermodilution curve is illustrated in Fig. 1. Two curves are shown in the picture, and both represent the difference between the blood temperature during the thermodilution process and the normal blood temperature. The stepwise curve shown in the figure shows an idealized approximation of the thermodilution curve, for an ejection fraction of 0.5 (i.e., in each cycle, the heart pumps half of the blood volume that was in the ventricle in the end of the diastole). The curve has a stepwise behaviour because of the nature of the thermodilution signal. In the measurement process, a bolus of saline, at a temperature that is higher of lower from the blood temperature, is injected into the right atrium or into the right ventricle and mixes with the blood in the ventricle, causing its temperature to increase or to decrease. Then, the ventricular contraction happens, expelling half of the blood to the pulmonary artery, where the blood temperature is measured by the thermistor. Then, the contractions end, and the ventricle starts to fill again. Since the ejection fraction is 0.5, the temperature of the mixture falls to half of its previous value. As the next contractions happen, in each contraction the temperature will fall to half its previous value. Thus the ideal thermodilution curve is composed by a series of plateaux. Suppose that the temperature of one of these plateaux is T_n, and the temperature in the plateau before this contraction is T_{n-1}. Then, it is easy to show, using thermodynamics [2], that the ejection fraction can be estimated

***Corresponding author*: Maxwell D. B. Melo,**
Federal University of Tocantins, Faculty of Electrical Engineering, Palmas, Brazil

by EF=1-T_n/T_{n-1}. Moreover, it is easy to show [2] that the cardiac output is approximately equal to a constant divided by the area under this curve. The second curve shown in Fig. 1 is the temperature that is measured by the thermistor probe embedded in the thermodilution catheter. This curve is a smeared version of the actual temperature curve, since the catheter has to be embedded into the catheter, and, because of that, it has a high thermal inertia, which causes the effect of a low pass filter. This distortion does not affect the measurement of the cardiac output, since the filtered curve keeps the same area as the undistorted curve. However, since the plateaus disappear, it is not possible to estimate the ejection fraction. G. N. Stewart articulated basic principles of the thermodilution method [3], attesting that if a substance were introduced at a constant rate into the bloodstream, it would be mixed with the blood, and if its concentration was measured at a point a little distant from the injection site, its decay rate would be inversely proportional to the rate of blood flow. A Swan-Ganz catheter is inserted into the human body through a peripheral vein and advanced to the right side of the heart, traversing the right atrium and right ventricle until it finally reaches the pulmonary artery.

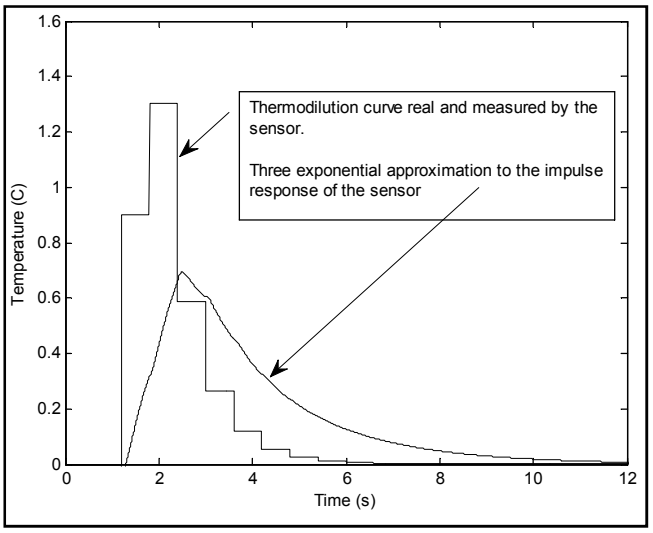

Fig. 1. Simulated Thermodilution curves – the idealized curve is modelled as a sequence of plateaus, and the measured curve can be approximated by the convolution of the idealized curve with the impulse response of a catheter that is approximated by a sum of real negative explonentials

The algorithm developed in this work can be implemented by the following sequence:

1. Acquisition of the thermodilution signal and the electrocardiogram.
2. Definition of the limits of the plateaus of the thermodilution curve by means of electrocardiogram R waves detection (the borders of the plateaus match with the instants of occurrence of R waves).
3. Assume an initial hypothesis for the values of the coefficients a, B, b, C, c, D and d. Using more realistic values makes the algorithm a little faster, but it is not a necessary condition.
4. Determine, from the borders, the midpoints of each plateau.
5. Calculate the position, in the vector, of the extreme and average points in each plateau of Figure 1 in the ideal curve is shown as a plateaus confluence.
6. Start of the iterative process, i.e. a loop of repetition for the approximation sequence.
7. Calculation of the impulse response of the catheter with four exponential components.
8. Performe the deconvolution of the signal using the current estimates of a, B, b, C, c, D, and d.
9. Calculation of the error function (which quantifies how close the sum of the absolute values of the inclinations of the portions of the final half of the first four plateaus is near zero).
10. For each separate coefficient, use a "delta" of 0.05, to determine the direction of the gradient in the downward direction on the surface.
11. Update of the new parameter estimates, in the decreasing direction of the gradient.
12. If the current error is less than 0.001, stop, and go to step 14.
13. Return to step 7.
14. Do the final deconvolution, showing the resulting graph.
15. Calculate the ejection fraction based on the final result of the deconvolution.

The error function, used in the iterative process, is given by the following relation,

$$error\_plateau = \sum_{meio}^{fim} \left| T\_dec\_aprox - \frac{\sum_{midle}^{end} T\_dec\_aprox}{vector\_size} \right| \quad (1)$$

where error_plateau is the error between the actual and deconvolved temperature and T_dec_aprox *(°C)* is the temperature signal obtained with the deconvolution of the signal using the approximate response with four exponentials. In step 8, the degree of deconvolution must be controlled according to the signal-to-noise ratio of the temperature signal captured by the slow sensor. Typically, the degree of deconvolution is limited by a low-pass filter IIR (Infinite Impulse Response) of order 2 and cutoff frequency of 10 Hz. As discussed in [4], if the noise level is very high, the cutoff frequency must be decreased until reaching an acceptable noise level. In step 15, the ejection fraction was calculated, in the simulations performed, by two different methods. In the first, the ejection fraction is estimated by the equation EF = 1-Tn / Tn-1, where Tn and Tn-1 are two successive plateaus. For the calculation, the first three successive pairs of plateaus are used which occur immediately after the peak of the thermodilution wave, and, after calculation, the means of the three calculations are calculated. The process of calculating the mean decreases the natural variability between successive beats. Also, there is always a small error associated with the first pair of plateaus, since the first plateau may in some cases still contain a small amount of the original injectate, so that the exponential decay phase may not yet have been effectively initiated. Averages also decrease this error. A flow diagram for this algorithm is shown in Figure 2.

Deconvolution of signals: Convolution is a mathematical way of combining two signals to form a third signal. It is the most important mathematical operation in digital signal processing. Using the strategy of superposition of impulse functions, systems can be described by a mathematical expression. Convolution is important because it relates the three signals of

interest [5, 6]. The deconvolution is the inverse of the convolution operation. In a commonly used approach to perform this operation, the input signal is obtained through a mathematical solution involving the Fourier transform of the input and output signals. This section describes the method used in this work. The output of a linear time-invariant (LTI) system can be represented as the convolution of an input signal with the impulse response of the system, as shown in equation (2), in the time domain.

$$T_{measured}(t) = h(t) * T_{real}(t) \quad (2)$$

where $T_{measured}(t)$ is the temperature signal measured by the thermistor probe (with a low pass effect) in the time domain, $h(t)$ is the impulse response of the sensor, and $T_{real}(t)$ is the undistorted temperature being measured. The asterisk represents the convolution operation. In the frequency domain, Eq. (2) becomes a point by point multiplication, as shown in Eq. (3).

$$T_{measured}(j\omega) = H(j\omega).T_{real}(j\omega) \quad (3)$$

In Eq. (3), $T_{measured}(j\omega)$ is the Fourier Transform (FT) of the measured signal, $H(j\omega)$ is the FT of the sensor impulse response, and $T_{real}(j\omega)$ is the FT of the temperature being measured. In this work, the FFT is approximated by the Fast Fourier Transform (FFT). The deconvolution [7, 8, 9] can be obtained by using the FFT of the impulse response of the system and the FFT of the measured signal. Equations (2) and (3) indicate that the temperature measured by the sensor corresponds to the convolution between the actual temperature and the impulse response of the sensor. The point by point division of the FFT of the signal measured by the FFT of the impulse response of the system is, in the idealized case, the basis of the deconvolution method proposed in this paper [10,11]. The deconvolution process is illustrated in Fig. 3. In the figure, $T(j\omega)$ is the FFT of the real temperature, $T_{meas}(j\omega)$ is the FFT of the measured temperature, and $N(j\omega)$ is the noise that is added due to interference, electronic noise and imprecision in the approximation for $H(j\omega)$. The sensor transforms the input $T(j\omega)$ into $H(j\omega)T(j\omega)$ plus the added noise. To perform the deconvolution, the measured signal is divided by $H(j\omega)$. The result is the recovered signal, $T_{meas}(j\omega)$, plus the noise divided by $H(j\omega)$ (or equivalently, multiplied by an inverse filter, $H_{inv}(j\omega)=1/H(j\omega)$. Since $H(j\omega)$ has an increasingly low amplitude as frequency increases, the high frequency components of the noise are greatly increased, generating an amount of noise that can render the $T_{meas}(j\omega)$ useless. Thus, a last stage with a third order low-pass filter is used to attenuate this noise component.

In the proposed method, the digitized versions of the actual and the measured temperatures, which will be called, from now, $x(t)$ and $y(t)$, and the impulse response of the temperature sensors ($h(t)$) are used, and they are named $x[n]$, $y[n]$ and $h[n]$. For discrete systems that are LTI, the convolution operation can be expressed by equation (4),

$$y_n = \sum_{m=0}^{N-1} h_{n-m} x_m \,, \quad (4)$$

where n and m are digital versions of the time variable, x_n is the digital version of the actual temperature being measured (which is not known yet and must be estimated by a deconvolution operation), h_n is the digital version of the impulse response of the system, and y[n] is the digital version of the output signal. N is the length of these three signals.

Eq. (4) can be re-written using matrix notation, as shown in Equation (5).

$$[y] = [h][x] \quad (5)$$

Where [y] is the system output vector, [h] is the Toeplitz matrix representing the discrete convolution and [x] is the discrete input vector.

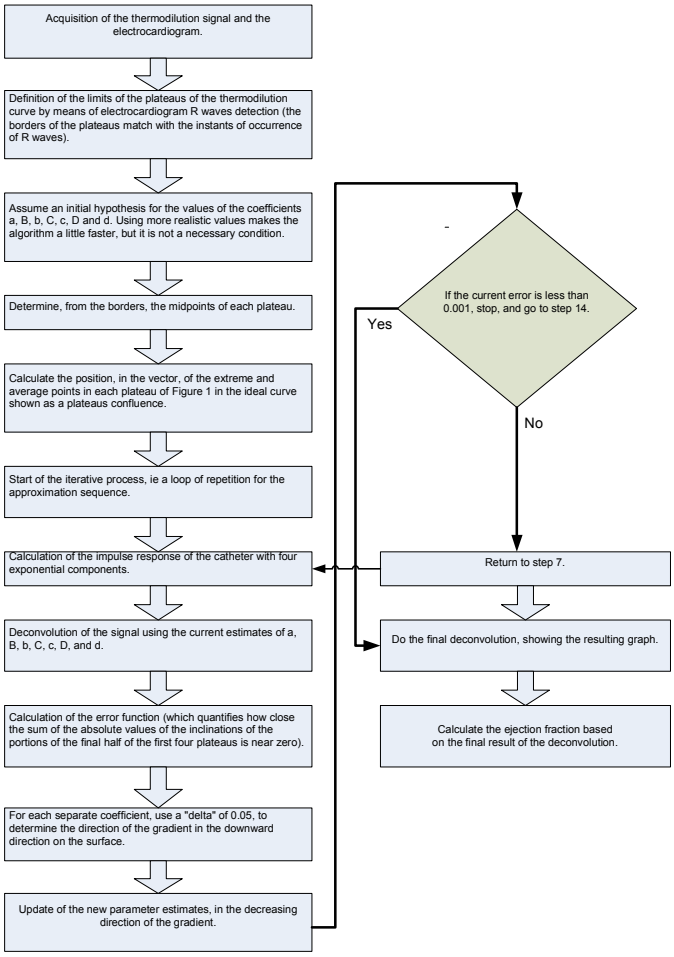

Fig. 2. Flow chart describing the Algorithm proposed in this work. The doal of the algorithm is to minimized an error function, which is defined by the sum of hte absolute values of the deconvolved curve. The convoution processe follows the steps presented in the chart

In this case, M = N, and the exact expression is shown in Equation (6). The proposed deconvolution method is shown in Fig. 3.

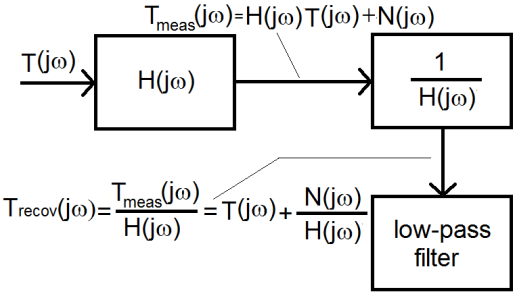

Fig. 3: Block diagram illustrating the basic building blocks of the proposed deconvolution method, using frequency domain

notation. T(jω) is the FFT of the real temperature, $T_{meas}(j\omega)$ is the FFT of the measured temperature, and N(jω) is the noise that is added due to interference, electronic noise and imprecision in the approximation for H(jω). The sensor transforms the input T(jω) into H(jω)T(jω) plus the added noise. To perform the deconvolution, the measured signal is divided by H(jω). The result is the recovered signal, $T_{meas}(j\omega)$, plus the noise divided by H(jω). Since H(jω) has an increasingly low amplitude as frequency increases, the high frequency components of the noise are greatly increased, generating an amount of noise that can render the $T_{meas}(j\omega)$ estimate useless. Thus, a last stage with a low-pass filter is used to attenuate this noise component.

$$\begin{bmatrix} y_0 \\ y_1 \\ y_2 \\ y_3 \\ \bullet \\ \bullet \\ y_{N-4} \\ y_{N-3} \\ y_{N-2} \\ y_{N-1} \end{bmatrix} = \begin{bmatrix} h_0 & 0 & 0 & 0 & \bullet\bullet\bullet & 0 & 0 & 0 & 0 \\ h_1 & h_0 & 0 & 0 & \bullet\bullet\bullet & 0 & 0 & 0 & 0 \\ h_2 & h_1 & h_0 & 0 & \bullet\bullet\bullet & 0 & 0 & 0 & 0 \\ h_3 & h_2 & h_1 & h_0 & \bullet\bullet\bullet & 0 & 0 & 0 & 0 \\ & & & & \bullet\ \bullet\ \bullet & & & & \\ & & & & \bullet\ \bullet\ \bullet & & & & \\ h_{M-7} & h_{M-8} & h_{M-9} & h_{M-10} & \bullet\bullet\bullet & h_0 & 0 & 0 & 0 \\ h_{M-3} & h_{M-4} & h_{M-5} & h_{M-6} & \bullet\bullet\bullet & h_1 & h_0 & 0 & 0 \\ h_{M-2} & h_{M-3} & h_{M-4} & h_{M-5} & \bullet\bullet\bullet & h_2 & h_1 & h_0 & 0 \\ h_{M-1} & h_{M-2} & h_{M-3} & h_{M-4} & \bullet\bullet\bullet & 0 & h_2 & h_1 & h_0 \end{bmatrix} \begin{bmatrix} x_0 \\ x_1 \\ x_2 \\ x_3 \\ \bullet \\ \bullet \\ x_{N-4} \\ x_{N-3} \\ x_{N-2} \\ x_{N-1} \end{bmatrix}$$

The problem of deconvolution can be seen as finding the inverse solution of the linear system proposed by equation (5). Thus, to perform the deconvolution it is necessary to find the vector x such that,

$$[x] = [h]^{-1}[y] \tag{7}$$

Where $[h]^{-1}$ is the inverse Toeplitz matrix.

In matrix notation, the FFT of a digital signal can be calculated by multiplying the matrix W, shown in Equation (8) by the digitized signal.

$$[W] = \frac{1}{N}\begin{bmatrix} 1 & 1 & 1 & \dots & 1 \\ 1 & W^{-1} & W^{-2} & \dots & W^{-(N-1)} \\ 1 & W^{-2} & W^{-4} & \dots & W^{-2(N-1)} \\ \vdots & \vdots & \vdots & \vdots & \vdots \\ 1 & W^{-(N-1)} & W^{-2(N-1)} & \dots & W^{-(N-1)^2} \end{bmatrix} \tag{8}$$

where $W = e^{-j\frac{2\pi}{N}}$. By multiplying both sides of Eq. (5) by the W matrix, we obtain Eq. (9),

$$\begin{aligned} &[W][y] = [W][h][x] \Leftrightarrow \\ &[W][y] = [W][h][W]^{-1}[W][x] \Leftrightarrow [Y] = [H][X], \end{aligned} \tag{9}$$

where the W^{-1} matrix is the complex conjugate matrix of W. It is not difficult to show that $[W].[h].[W]^{-1}$ is a diagonal matrix. Therefore, in the frequency domain, Eq. (10) must be solved:

$$X_r = [H]^r.[Y], \tag{10}$$

where $[H]^r$ is a diagonal matrix whose elements are the reciprocals of the corresponding elements of the [H] matrix. An advantage of using the DFT is to avoid a matrix inversion operation that it is often slow in the time domain, using a more efficient algorithm in the frequency domain. After calculating the recovered signal in the frequency domain [X_r *(j*w)] the recovered signal in the time domain [$x_r(t)$] can be obtained by calculating its inverse Fourier transform (in this case, this function can be approximated by the inverse Fast Fourier Transform (IFFT) of the FFT of the recovered signal). The result that is obtained is always noisy, and it needs to be filtered. In the proposed method, the filter used is a digital 3rd order Butterworth IIR filter, whose cutoff frequency is optimized through an iterative process. The proposed system can be modelled by a temperature sensor based on a thermistor whose impulse response can be approximated by a sum of one or more exponential signals. The process will now be illustrated using the h[n] function in equation (11).

$$h[n] = 2e^{-3n} + 3e^{-4n} + 5^{-8n} \tag{11}$$

The plot corresponding to h[n] is shown in Fig. 4, for a 10 seconds period, using a sampling period of 0.1 s (sampling frequency of 10 Hz). A unit step function, u(n-50), is shown in Fig. 5 (b). The convolution of the discrete signals of Figs. 4 and 5(b) is shown in Fig. 5(a). By applying these equations, using the Toeplitz matrix, the convolution has been calculated and it is shown in Fig. 5 (a), which corresponds to the step response of the thermistor. In practice, intrinsic noise is very common in instrumentation systems, due to several physical effects. To simulate this situation, Gaussian noise is added to the output y[n], as illustrated at the top of Fig. 6(a). The noise has zero mean and standard deviation equals to zero [11]. The deconvolution process described by Equations (9) and (10), and by using the Butterworth filter is illustrated in Figure 6(b). It is clearly seen that a small amount of noise can distort the deconvolution operation. A more realistic model for the response of a thermistor probe embedded in a catheter can be obtained by an approximation using three exponential components, as shown in Equation (11) [2, 8, 11, 12, 13, 14, 15] and applied in this paper:

$$h(t) = K\left(e^{-at} + B.e^{-bt} + C.e^{-ct}\right), \tag{11}$$

where *h(t)* is the impulse response, a, B, b, C, c are parameters obtained in the characterization of the sensor, and K is a constant that is set such that the area under *h(t)* is equal to 1, which is:

$$K = \frac{1}{\frac{1}{a} + \frac{B}{b} + \frac{C}{c}} \tag{12}$$

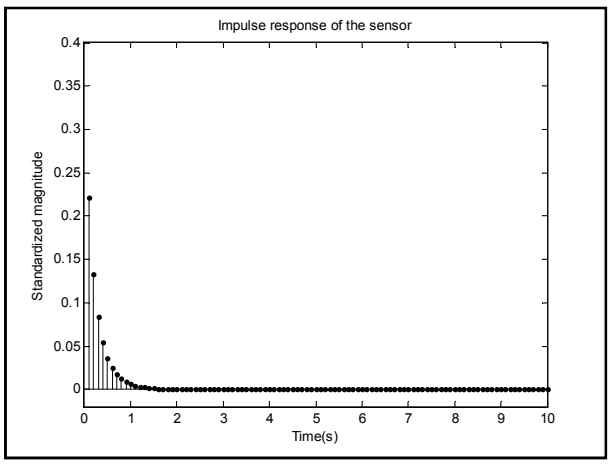

Fig. 4. Impulse response to the system under analysis. For the system under analysis in this section, we assume a response that is a sum of exponential components

Fig. 6(a) shows an example of a measured step response with a small amount of noise added. The deconvolution process was applied, and the result is shown in Fig. 6 (b). It is possible to see, in Fig. 6, that when a small amount of noise is added to the measured signal, the deconvolved signal can get noisy. In this example, the amount of noise in the deconvolved noise is not too high, but, for higher noise levels it can get very high, making the result unreadable. In this case, the cut-off frequency of the filtering process must be decreased, and there will be a trade-off between the amount of noise and the quality of the recovered signal.

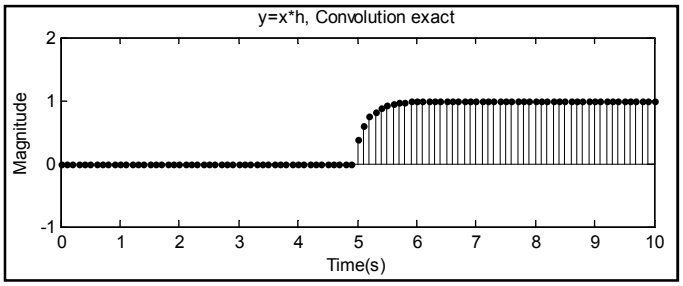

(a)

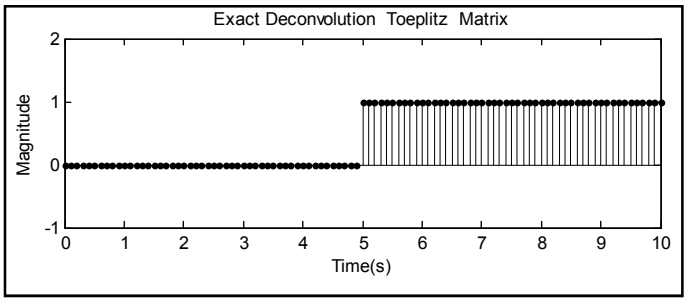

(b)

Fig. 5. Convolution (upper curve) and deconvolution (lower curve) for the system under analysis. The convolution (y [n] = h [n] * x [n]) for the system under discussion is shown in the upper curve, and the deconvolution is shown in the lower part of the curve. Note that, if there is no noise, the deconvolution is accurate

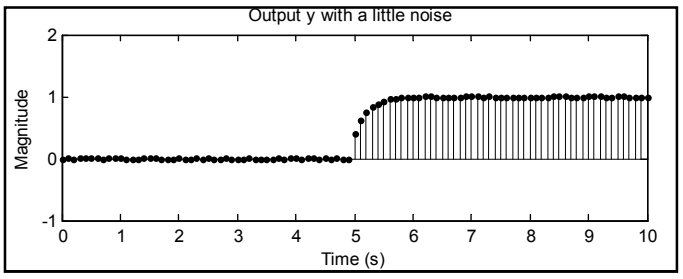

(a)

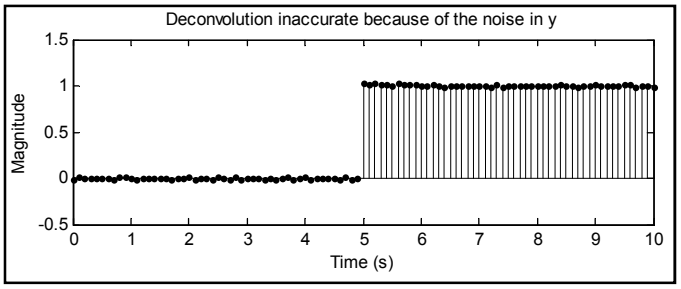

(b)

Fig. 6. Sensor output resulting from the measurement of the temperature shown in Fig. 6 is shown in (a). The result of the deconvolution operation is shown in Fig. 6 (b)

A small amount of noise can greatly distort the deconvoluted signal. The result for a slightly higher noise in y [n] is shown in Figure 6 (b). It is seen from the figure that the deconvolved time signal presents noticeable distortion. The deconvolution process described is the main part of the process that is proposed in this paper for deconvolution of the thermodilution curve. The other part is described as follows. There is one characteristic that is observed in the true temperature signal x(t): during the decaying period, the curve has plateaux, and the slopes of these plateaux are close to zero. Thus, the algorithm for estimation of h(t) and for deconvolution of the thermodilution curve works as follows: (i) an initial estimate of the six parameters (a, B, b, C, c, and the cut-off frequency of the third order Butterworth filter), of h(t) is chosen; (ii) perform the deconvolution operation, obtaining a deconvolved curve; (iii) estimate the curve slope at the center of the three first plateaux in the descending curve, and add their values, obtained the sum of the slopes, SS (the goal is to minimize this values); (iv) run 5 new convolution operations, by changing, in each one, only one of the five parameters, and, using the values of the obtained SS values to estimate the direction of the descending gradient; (v) based on the gradient direction, change the six parameters slightly, calculating the new value of SS; (vi) if the new value is smaller than a chosen value, stop the search, and go to step (vii), if not, go back to step (ii); (vii) using the final parameters, perform the final deconvolution operation, and calculate the ejection fraction and the end diastolic volume. In order to test the effectiveness of the method, we performed mathematical simulations, and tests with Swann-Ganz catheters installed in the mock circulatory system described in [2]. The acquisition system shown in Fig. 7 has been developed to allow the measurement and processing of the thermodilution signal measured with Swann-Ganz catheters.

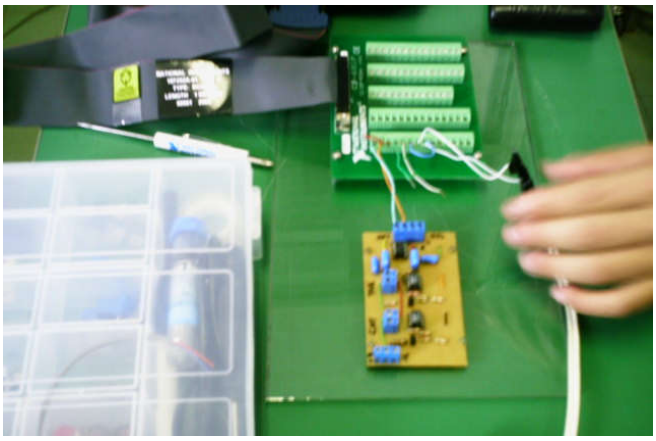

Fig. 7. Data acquisition system to obtain the thermodilution curves

RESULTS

Several mathematical simulations were performed in the Matlab environment in order to assess the effectiveness of the method. Fig. 8 shows the results of simulations in which the actual ejection fraction ranged from 0.1 up to 0.9, with intervals of 0.1, and the heart rate ranging from 10 up to 290 beats per minute (BPM), with intervals of 10 bpm. The standard deviation of the Gaussian noise added to the signal, in the simulation was 0.02 ^{o}C. The computer simulations showed the limits of the proposed algorithms: the algorithm is not satisfactory operation for heart rates above 200 and ejection

fractions above 0.8. There are two reasons for the failure of the algorithm for high heart rates and higher ejection fractions.

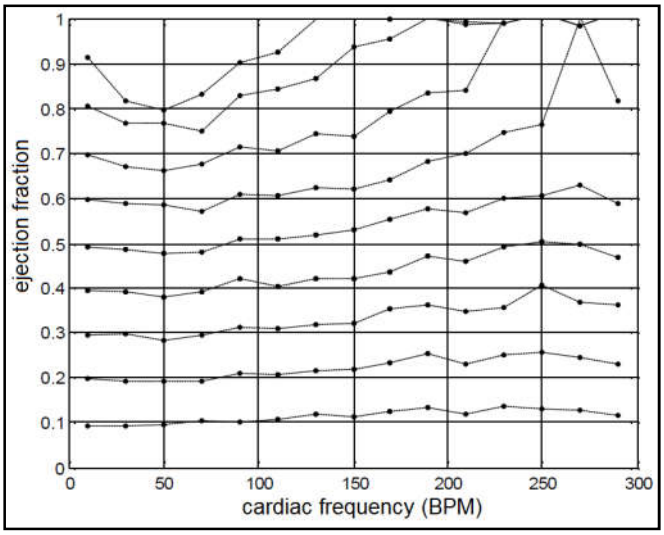

Fig. 8. Results of the computational simulation. The actual ejection fraction ranged from 0.1 up to 0.9, with intervals of 0.1, and the heart rate ranging from 10 up to 290 beats per minute (BPM), with intervals of 10 bpm. The standard deviation of the Gaussian noise added to the signal, in the simulation was 0.02 ^{o}C

The first reason is that, for high ejection fractions, the fall after each plateaux is too abrupt, and at the first stroke, the curve drops to 10% of its value, and second, to 1%. Thus, the algorithm does not have the number of reference points required for deconvolution. It is important to note, however, that even the expensive systems with very fast sensors allow the measurement of ejection fractions only up to 0.7. The reasons for this limitation are as follows: the first plateau has a fall to just over 30%, the second to 9%, 3% the third and fourth 1%. In the first pair, which is the most accurate, the accuracy is impaired by the fact that immediately after the start of decay, there are still remaining mixture injection. The second and third pairs are inaccurate due to its small amplitude. Thus, this limitation is not only for the system with deconvolution, but also with the system with a fast sensor. Another reason for the error is that, for heart rates above 150, the limits of the plateaus are very close together, and the algorithm does not have strong points of reference to calculate the plateau slope at the centre of the plateau, and this shortcoming impairs the effectiveness of the algorithm. This is a fundamental limitation of the algorithm herein propose that, perhaps, may be resolved in future developments. A possible future development is the adaptation of this deconvolution algorithm to the continuous measurement systems, which use resistive heating of the blood (Yelderman, 2004). The simulations using the Swann-Ganz catheter in the mock circulatory system were performed by acquiring both the temperatures measured by the slow sensor embedded in the catheter and a very fast sensor specially built for this purpose. Then, the ejection fraction was calculated by using both curves. The results comparing these two measurements are presented in Table 1.The table have shown that the measurements made with the enhanced signal from the thermodilution catheter had a mean error of 8.90%, where bpm is beats per minute and EF is the ejection fraction. This level of errors in both the simulations and the measurements had about the same magnitude as the errors in previous works [2][8][9]. However, the processing time required for the experiments were much lower for the algorithm herein presented.

Table 1. Results comparing the measurements of ejection fraction by a fast sensor and the signal from a slow sensor that was enhanced by the deconvolution method

Cardiac rate (bpm)	EF with the fast sensor	EF with the algorithm	Error (%)
22.5	0.28	0.31	10.7%
25.2	0.26	0.29	11.5%
21.88	0.20	0.21	4.5%
27.87	0.46	0.50	6.7%
32.83	0.34	0.32	6.9%
31.35	0.19	0.21	10.0%
38.92	0.32	0.36	12.5%
38.71	0.22	0.23	8.9%
63.57	0.44	0.47	4.2%
mean error			8.90%

Conclusions

The proposed algorithm uses a principle that is different from the ones used in previous works, combining both frequency domain and time domain techniques. This work presents the proposal and the test of a system that allows the enrichment of thermodilution signals captured with slow temperature sensors. In the computational simulations and experimental tests with the mechanical simulator, the test worked very well, presenting errors less than 10%. The effort and computational time was much lower than those presented in the literature. The time needed to process the data in the proposed algorithm was around 9 seconds, in the worst case. Thus, the method has very good potential for future use. However, it still needs further development, including the test in animal models, and, later, in human subjects.

REFERENCES

Bickle, L. W., 1971. "A time domain deconvolution technique for the correction of transient measurements," Report SC-RR-71 06658, Sandia Laboratories, Albuquerque, New Mexico, Exploratory Measurements Division 1442, November.

da Rocha, A. F. 1997. "The Dynamic Behavior of Thermistor Probes", Dissertation for degree of Doctor of Philosophy, University of Texas, Austin, May.

da Rocha, A. F.; dos Santos, I.; Nascimento, F. A. O. & de Melo, M. D. B. 2005. Dieter Haemmerich and Jonathan W Valvano, "Effects of the time response of the temperature sensor on thermodilution measurements", Physiol. Meas. 26.

Dantzig, J. A. 1985. "Improved transient response of thermocouple sensors," Rev. Sci. Instrum., v. 56, no. 5, pp. 723-725.

de Melo, M. D. B. 2007. Algoritmo para Recuperação de Sinais de Temperatura de Cateteres de Artéria Pulmonar. Tese de Doutorado, Departamento de Engenharia Elétrica (ENE), Universidade de Brasília.

dos Santos, Í. 2000. Proposta de um método para medição da fração de ejeção do ventrículo direito, Dissertação (Mestrado em Engenharia Biomédica), Departamento de Engenharia Elétrica, Universidade de Brasília, Brasília.

Hori, J.; Saitoh, Y. & Kiryu, T. 1994. "Improvement of the time-domain response of a thermodilution sensor by the natural observation system," IEICE Trans. Fundamentals, v. E77-A, n. 5, may.

M. D. B. Melo, H. X. Araujo and A. F. da Rocha. A Novel Methodology for Signal Recovery in Lin.ear Time Invariant Systems for Medicine Applications. PRZEGLĄD ELEKTROTECHNICZNY, ISSN 0033-2097, R. 92 NR 10/2016.

Mouncastle, Vernon B., "Medical hysiology", Copyright 1974 by The C. V. Mosby Company.

Novato, Luciana Rabelo, "Projeto e Implementação de um Sistema de Termodiluição Baseado em Labview", Projeto Final de Graduação em Engenharia Elétrica, Departamento de Engenharia Elétrica, UnB, 2004.

Oppenheim, Alan V., Schafer, Ronald W., "Discrete-Time Signal Processing", Pretice-Hall International, Inc, 1989.

Riad, S., M., "The deconvolution problem: an overview," Proceedings of the IEEE, v. 74, pp. 82-85, January 1986.

Salgado, C. R., Galletti, P. M., "In vitro evaluation of the thermodilution technique for the measurement of ventricular stroke volume and End-Diastolic Volume," *Cardiologia*, vol. 49, n.2, pp. 65-78, 1966.

Smith, S. W., The Scientist and Engineer's Guide to Digital Signal Processing, Second Edition. www.dspguide.com

Trautman, E. D., Newbower, R. S., "The development of indicator-dilution techniques," IEEE Transactions on Biomedical Engineering, vol. BME-31, n. 12, December, 1984.

Yelderman, Mark, M.D. CEO, Monterey Medical Solutions, CA, USA, "Continuous Measurement of Cardiac Output Using Stochastic System Identification Techniques", Proceedings of the 26th Annual International Conference of the IEEE EMBS, San Francisco, CA, USA • September 1-5, 2004.

****